ISSN 2278-3091
Volume 8, No.1.6, 2019
International Journal of Advanced Trends in Computer Science and Engineering
Available Online at http://www.warse.org/IJATCSE/static/pdf/file/ijatcse2381.62019.pdf
https://doi.org/10.30534/ijatcse/2019/2381.62019

# Moth-Flame Optimization Algorithm with Different Course for Optimal Photovoltaic Location and Sizing

**Syahirah Abd Halim[1,3], Hazwani Mohd Rosli[2], Husna Farzana Hasri[3]**
[1]Centre for Integrated Systems Engineering
and Advanced Technologies, Faculty of Engineering & Built Environment, Universiti Kebangsaan Malaysia, Malaysia, syahirah_h@ukm.edu.my
[2]School of Engineering, Asia Pacific University of Technology & Innovation, Malaysia, hazwani@staffemail.apu.edu.my
[3]Electrical and Electronic Engineering Programme, Faculty of Engineering & Built Environment, Universiti Kebangsaan Malaysia, Malaysia, husnafarzanahasri@gmail.com

## ABSTRACT

The increasing usage of photovoltaic (PV) sources for electricity power generation as well as the recent advancement in PV technology offers a promising solution to conventional energy issues. However, high penetration of PV may give negative impacts on the operation of distribution feeders due to intermittent nature of its generation ability. Therefore, optimal design of PV sources is essential to support the grid voltage regulation and improve the performance of the distribution network. In this study, Moth-Flame Optimization (MFO) algorithm with different spiral course technique was applied for optimizing the location and size of different PV generation units to improve the voltage profile and minimize the total active power loss, subjected to the system operational constraints. The initial system power loss was determined by using distribution load flow analysis based on the backward-forward technique. The MFO algorithm with different spiral course was then implemented to determine the optimal placement and sizing of the PV in the IEEE 12 and 33-bus radial distribution networks. The performance of the MFO algorithm with different spiral course was then analyzed based on the convergence characteristics. The results prove that installing PVs at optimal location with appropriate sizing could minimize the total real power loss and improve the voltage profile of the tested distribution network.

**Key words:** Active power loss, grid-connected photovoltaic system, Moth-Flame Optimization, spiral course.

## 1. INTRODUCTION

Distribution systems are commonly connected in radial due to simplicity of network arrangement and low initial cost of equipment. Radial distribution networks are fed to substation and receives power from the centralized generating stations through the interconnected transmission network. However, the radial distribution networks normally have high R/X ratio, which can result in high power losses and voltage instability. Therefore, distributed generations (DGs) have been employed to overcome the drawbacks of the radial distribution network in order to improve the system reliability and voltage regulation [1], [2]. With the increasing demand for efficient and reliable electricity supply, the issues involving DG applications in the distribution system network has drawn remarkable attention worldwide.

Distributed generation is a small-scale electricity power generator typically generate electricity at between 1 kW and 50 MW. DG produces electricity power at a site close to the load center or that are tied to an electrical distribution system. DG units can be energized by both renewable and non-renewable sources. DG provides many advantages towards the operation and technical aspect of distribution system in terms of the system reliability, voltage profile and power quality improvement [3]-[5]. Recent advancement such as photovoltaic (PV) based distributed generations offers a promising solution to conventional energy issues such as price fluctuations of diesel fuel and high emission of carbon dioxide [6], [7]. Furthermore, the implementation of grid connected PV sources in distribution network also contribute in strengthening the overall system efficiency and enhances the peak load capacity.

However, improper placement and sizing of the grid connected PV will significantly affect the technical aspects of the distribution network in term of power quality degradation, system voltage instability and power losses [8]-[10]. Therefore, optimum placement and sizing of the PV based distributed generation in the distribution network is very crucial to achieve the power losses reduction and voltage profile improvement [11], [12].

The selection of optimal location and size of PV system in a radial distribution network involves complex optimization problems. Various meta-heuristic optimization techniques have been proposed to determine the optimal inclusion and size of the PV in the distribution network such as Differential Evolution (DE), Evolutionary Programming (EP), Particle Swarm Optimization (PSO) and Genetic Algorithm (GA) [13]-[16]. Additionally, hybrid techniques have also been widely used to find the optimal PV application, which include Genetic Algorithm and Improved Particle Swarm Optimization (GA-IPSO), Ant Colony Optimization and Artificial Bee Colony (ACO-ABC) and Modified Shuffled Frog Leaping Algorithm and Differential Algorithm (MSFLA-DE) [17]-[19].

In this study, a new technique based on the optimal sizing and placement of photovoltaic system in a radial distribution network is proposed. With the aim of minimizing the active power losses and voltage instability, Moth-Flame Optimization (MFO) will be utilized to solve the optimization problem by considering the equality, inequality and security constraints. The algorithm has demonstrated its capability in providing consistent and robust solution for various power system optimization problems. In the application of optimal sizing and placement of the PV system for loss minimization, the proposed MFO technique is capable of solving the nonlinear optimization problem with higher accuracy and reduced computational time.

## 2. METHODOLOGY

Moth-Flame Optimization (MFO) algorithm with different spiral course technique was implemented to determine the optimal placement and sizing of grid-connected PV system for active power loss reduction and voltage profile improvement in radial distribution networks. Two case studies were analyzed based on the IEEE 12 and 33-bus radial distribution network to validate the performance of the proposed method using MATLAB software.

### 2.1 Objective Function and Constraint

An efficient distribution network operation requires minimization of the total active power losses. Single-objective optimization problem considering the system operational constraints has been formulated to find the optimal location and size of the PV system by minimizing the total active power losses for all lines in the radial distribution networks. The losses in the system can be calculated by (1).

$$P_{Loss} = \sum_{i=1}^{N} \sum_{j=1}^{N} X_{ij} \left( P_i P_j + Q_i Q_j \right) + Y_{ij} \left( Q_i P_j + P_i Q_j \right) \quad (1)$$

$$X_{ij} = \frac{RL_{ij} \cos\left(\delta_i - \delta_j\right)}{V_i V_j} \quad (2)$$

$$Y_{ij} = \frac{RL_{ij} \sin\left(\delta_i - \delta_j\right)}{V_i V_j} \quad (3)$$

where $P_i$ is the net active power injection at bus $i$, $Q_i$ is the net reactive power injection at bus $i$, $RL_{ij}$ is the line resistance between bus $i$ and $j$, $V_i$ is the voltage at bus $i$ and $\delta_i$ is the angle at bus $i$.

The objective function to minimize the total real power loss in the radial distribution networks can be expressed as in (4):

$$OF_{Min} = P_{Loss} = \sum_{k=1}^{N_S} Loss_k \quad (4)$$

Subjected to the following system constraints:

Power balance constraint,

$$\sum_{i=1}^{N} P_{DG_i} = \sum_{i=1}^{N} P_{R_i} + P_{Loss} \quad (5)$$

Voltage constraint,

$$|V_i|\min \le |V_i| \le |V_i|\max \quad (6)$$

Current limit,

$$|I_{ij}| \le |I_{ij}|\max \quad (7)$$

where, $OF_{Min}$ is the objective function, $P_{Loss}$ is the active power loss in the system, $Loss_k$ is the distribution loss at section $k$, $N_s$ is the number of sections, $P_{DGi}$ is the active power generation of DG at bus $i$, $P_{Ri}$ is the power request at bus $i$.

### 2.1 Moth-Flame Optimization Algorithm for Optimal PV Location and Sizing

Moth-Flame Optimization (MFO) is a nature-inspired optimization based on transverse orientation of moths' navigation method [20]. The moths commonly fly at night by maintaining a fixed angle with respect to the moon. This navigation method provides a very effective way for the moths to travel in a straight line for long distances. However, the moths can be easily trapped in a deadly spiral course during the presence of artificial lights. This behavior is depicted in Figure 1 and can be mathematically formulated to solve for complex optimization problem.

In MFO algorithm, the moths are considered as the candidate

solutions while the position of the moths in the space is considered as the problem's variables. The moths are the actual search agents moving around the search space, which result in the actual solutions. Meanwhile, the flames are the best solutions obtained so far based on the position of the moths. Calculation and update of solution are then performed based on the number of moths. Different types of spiral functions can be utilized for the MFO formulations, which satisfy the following criteria [21]-[25]:

1. The initial point of the spiral should start from the moth.
2. The final point of the spiral should be the flame position.
3. Fluctuation of the range of spiral must be within the search space.

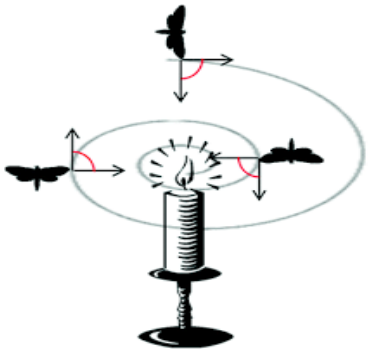

**Figure 1:** Moth-Flame Optimization Concept [21]

The MFO based approach for solving the optimal placement and sizing of the grid connected PV system in the radial distribution networks involves the following steps:

Step 1: The initial conditions for the optimization process were defined, which include line data, bus data, total generation limit, bus number limit, PV dimension, and maximum number of iterations. The set of moths representing the bus number for PV location and sizing can be initially described as the following matrix:

$$M = \begin{bmatrix} M_{1,1} & M_{1,2} & \cdots & M_{1,d} \\ \vdots & \vdots & \cdots & \vdots \\ \vdots & \vdots & \cdots & \vdots \\ M_{n,2} & M_{n,2} & \cdots & M_{n,d} \end{bmatrix} \quad (8)$$

where $n$ is the number of moths and $d$ is the number of variables (dimension). The corresponding active power loss was determined based on the initial position of the PV location and size using backward-forward method. The fitness values were then calculated for each moth and represented as the following matrix:

$$OM = \begin{bmatrix} OM_1 \\ \vdots \\ \vdots \\ OM_n \end{bmatrix} \quad (9)$$

where $n$ is the number of moths.

Step 2: The following flames matrix was then obtained by sorting out the moths according to their fitness values.

$$F = \begin{bmatrix} F_{1,1} & F_{1,2} & \cdots & F_{1,d} \\ \vdots & \vdots & \cdots & \vdots \\ \vdots & \vdots & \cdots & \vdots \\ F_{n,2} & F_{n,2} & \cdots & F_{n,d} \end{bmatrix} \quad (10)$$

where $n$ is the number of moths and $d$ is the number of variables (dimension).

The fitness values were then calculated for each flame and represented as the following matrix:

$$OF = \begin{bmatrix} OF_1 \\ \vdots \\ \vdots \\ OF_n \end{bmatrix} \quad (11)$$

where $n$ is the number of moths.

Step 3: The moth's position was then computed based on the lower limit and upper limit of the total bus number and maximum power generation from both grid and PV connection. Equation (12) was then used to update the position of each moth with respect to the flame.

$$M_i = S\left(M_i, F_j\right) \quad (12)$$

where $M_i$ is the $i$-th moth, $F_j$ is the $j$-th flame and $S$ is the spiral function.

Step 4: A logarithmic spiral function was selected as the first update mechanism of moths based on the following expression:

$$S\left(M_i, F_j\right) = D_i . e^{bt} . (\cos 2\pi t) + F_j \quad (13)$$

where $D_i$ is the distance of the $i$-th moth for the $j$-th flame, $b$ is a constant to define the shape of the logarithmic spiral, and $t$ is a random number between [-1, 1]. The $t$ parameter in the spiral equation defines the role of $t$ parameter, $t$ = -1 is the closest position to the flame, while $t$ = 1 shows the farthest. Equation (13) represents the spiral flying path of the moths,

in which the next position of a moth is usually defined with respect to a flame. This determine the best position and sizing of PV so far.

Several conditions need to be satisfied, where the initial point should start from the moth while the final point should be the flame position. Furthermore, fluctuation of the range of spiral must also be located within the search space. *D* was then calculated as in (14).

$$D_i = \left| F_j - M_i \right| \tag{14}$$

where $D_i$ is the distance of the *i*-th moth for the *j*-th flame, $F_j$ is the *j*-th flame and $M_i$ is the *i*-th moth.

Therefore, a hyper ellipse can be assumed around the flame in all directions whilst the next position of the moth would be within this space. To ensure successful exploration and exploitation of the search space, the spiral equation allows the moth to fly around the flame, but not necessarily in the space between them. The logarithmic spiral space is illustrated in Figure 2.

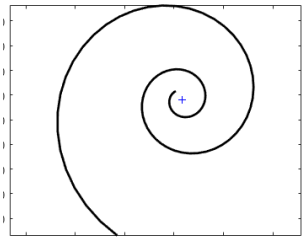

**Figure 2:** The logarithmic spiral

Step 5: The logarithmic spiral course was then determined based on the distance between the flame and the moth.

Step 6: The exploitation of the best PV location and sizing can be affected by the position updates of the moths with respect to different locations in the search space. To overcome this problem, an adaptive mechanism was utilized for each number of flames, represented by the following equation:

$$\text{flame no} = round\left( N - l \times \frac{N-1}{T} \right) \tag{15}$$

where *l* is the current number of iteration, *N* is the maximum number of flames, and *T* is the maximum number of iterations.

### 2.1.1 Hyperbolic Spiral

In order to improve the performance of MFO algorithm, a hyperbolic spiral course for the flying moths is considered. The hyperbolic spiral, also known as reciprocal spiral, is represented by a transcendental plane curve with an inversed center at the origin [8]. The initial point of the hyperbolic spiral starts at an infinite distance from the pole in the center and it winds faster around approaching the pole, as illustrated in Figure 3. Equation (16) represents the formulated MFO algorithm using the hyperbolic spiral.

$$S\left(M_i, F_j\right) = D_i . \frac{\cos\left(2\pi t\right)}{t} + F_j \tag{16}$$

where $D_i$ is the distance of the *i*-th moth from the *j*-th flame, *t* is a random number in [-1, 1] and $F_j$ is the *j*-th flame.

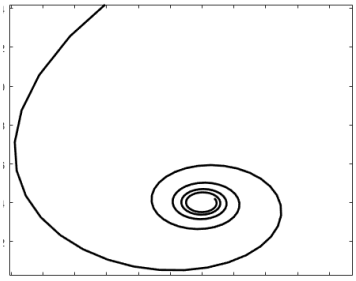

**Figure 3:** The hyperbolic spiral

### 2.1.2 Archimedes' Spiral

The Archimedes' spiral is another course for the flying moths to reach the flame. The spiral starts at the origin to form a curve with three rounds. As depicted in Figure 4, the distances of intersection points along the line through the origin are equivalent, which can be represented as a polar equation form (17).

$$r = a\theta^{\frac{1}{n}} \tag{17}$$

where *n* is a constant that determines how tightly the spiral is wrapped. Figure 4 represents the Archimedes' spiral using *n* = 1. Equation (18) represents the formulated MFO algorithm using the Archimedes' spiral.

$$S\left(M_i, F_j\right) = D_i . t . \cos\left(2\pi t\right) + F_j \tag{18}$$

where $D_i$ is the distance of the *i*-th moth from the *j*-th flame, *t* is a random number in [-1, 1] and $F_j$ is the *j*-th flame.

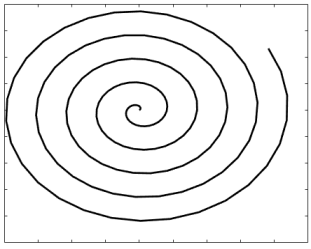

**Figure 4:** The Archimedes' spiral

## 3. RESULTS AND DISCUSSION

The single line diagram of the IEEE 12 and 33-bus network are illustrated in Figure 5 and Figure 6. The base kVA of the tested system is 10 kVA. The simulation parameters for the MFO algorithm are shown in Table 1. In this section, the performance analyses of different MFO algorithm with Logarithmic (MFO-L), Hyperbolic (MFO-H), and Archimedes (MFO-A) spirals considering optimal PV location and sizing were conducted.

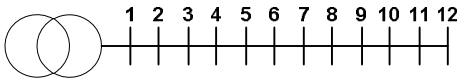


**Figure 5:** A single line diagram of 12-bus radial distribution network

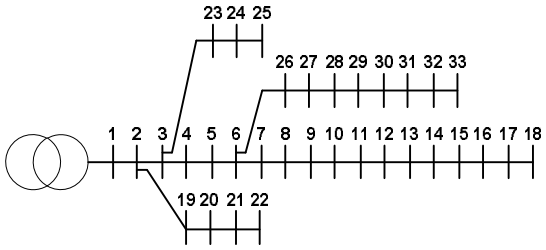


**Figure 6:** A single line diagram of 33-bus radial distribution network

**Table 1:** Parameters value for MFO algorithm with different spiral course

| Parameters | Value |
|---|---|
| Number of moths | 20 |
| Number of PV dimension | 1 |
| Number of iterations | 100 |
| Number of run | 10 |

In order to determine the robustness of MFO algorithm with different spiral course, consistency test was plotted in Figure 7 and Figure 8. The convergence characteristics are also provided in Figure 9 and Figure 10 to show the ability of different spiral techniques in converging towards the minimal value of fitness function. Both consistency and convergence characteristic tests conducted were based on one PV location and sizing for the IEEE 12 and 33-bus network.

As shown in Figure 7, MFO-H gives a consistent result at the lowest fitness value for every run compared to MFO-L and MFO-A. In Figure 8, MFO-H gives 9 out of 10 consistent results at the lowest fitness value as compared to MFO-L and MFO-A which gives 7 and 4 out of 10 consistent results respectively. Hence, it shows that MFO-H gives a better consistency result for the IEEE 12 and 33-bus network compared to MFO-L and MFO-A.

Figure 9 shows that MFO-H reaches minimum fitness at 8$^{th}$ iteration while MFO-L and MFO-A reaches minimum fitness at 13$^{th}$ and 17$^{th}$ respectively for the IEEE 12-bus network. Meanwhile in Figure 10, MFO-H reaches minimum fitness at 9$^{th}$ iteration while MFO-L and MFO-A reaches minimum fitness at 22$^{nd}$ and 17$^{th}$ iteration respectively for the IEEE 33-bus network. Therefore, MFO-H has demonstrated faster convergence characteristic as compared to MFO-L and MFO-A.

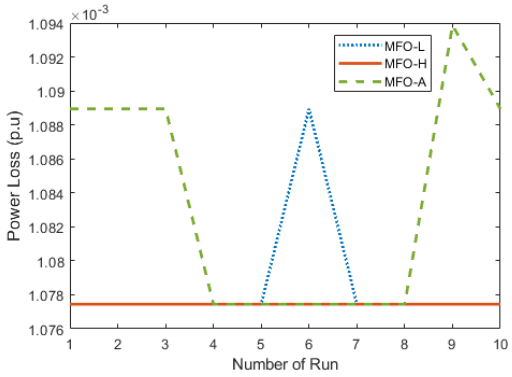


**Figure 7:** Consistency of MFO algorithms with different types of spiral for IEEE 12-bus network

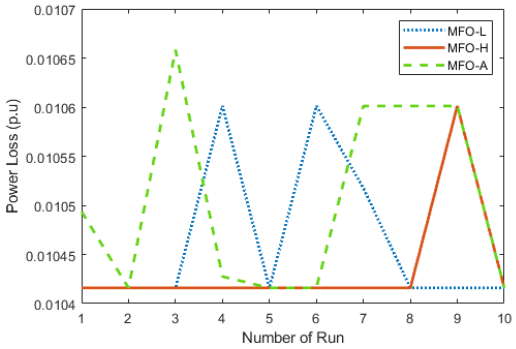


**Figure 8:** Consistency of MFO algorithms with different types of spiral for IEEE 33-bus network

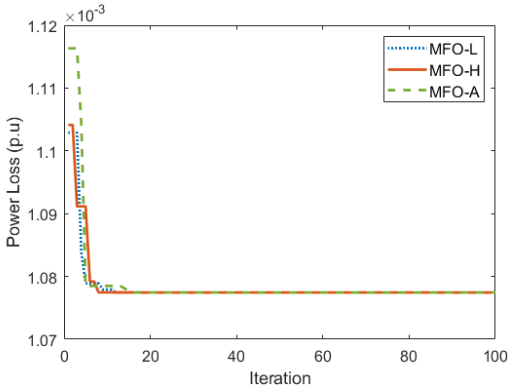


**Figure 9:** Convergence characteristic of MFO algorithms with different types of spiral for IEEE 12-bus network

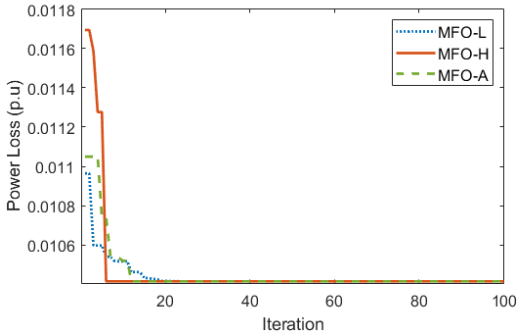


**Figure 10:** Convergence characteristic of MFO algorithms with different types of spiral for IEEE 33-bus network

According to the performance tests, it was found that all spiral techniques result in equivalent minimum fitness values of 0.001077 and 0.010415 for the IEEE 12 and 33-bus network respectively at 100$^{th}$ iteration. This shows that the optimum PV location and sizing obtained by three different spiral techniques are consistently similar. The different spiral techniques only affect the performance of MFO algorithm in terms of consistency and convergence characteristic. In which, MFO-H shows the best performance as compared to MFO-L and MFO-A.

The results obtained for optimal PV location and sizing are summarized in Table 2 and Table 3 accordingly. Note that, all three spiral techniques show similar minimum fitness or converge at the same minimum fitness. Hence, all three spiral course techniques give similar value of optimal PV location and sizing. Different number of location and sizing were tested using the MFO algorithm to analyze the network system performance based on the power loss reduction and system voltage profile.

**Table 2:** Optimal PV location and sizing for IEEE 12-bus network

| Number of PV | Total Power Loss (kW) | Power Loss Reduction | Optimal Size of PV (kW) | Optimal Location of PV |
|---|---|---|---|---|
| 0 | 20.7138 | - | - | - |
| 1 | 10.7744 | 47.98% | 235.5011 | Bus 9 |
| 2 | 9.4163 | 54.54% | 183.8582<br>137.7886 | Bus 7<br>Bus 10 |
| 3 | 9.1561 | 55.78% | 113.4182<br>132.8100<br>137.7885 | Bus 4<br>Bus 7<br>Bus 10 |

**Table 3:** Optimal PV location and sizing for IEEE 33-bus network

| Number of PV | Total Power Loss (kW) | Power Loss Reduction | Optimal Size of PV (kW) | Optimal Location of PV |
|---|---|---|---|---|
| 0 | 203.0812 | - | - | - |
| 1 | 104.1595 | 48.71% | 2575.5732 | Bus 6 |
| 2 | 86.0682 | 57.62% | 846.4083<br>1158.7255 | Bus 13<br>Bus 30 |
| 3 | 71.6293 | 64.73% | 788.1792<br>1093.3222<br>1057.9976 | Bus 13<br>Bus 24<br>Bus 30 |

Table 2 shows the implementation of optimal PV location and sizing for the IEEE 12-bus network system. Connecting one PV at Bus 9 with optimal generation of 235.5011 kW reduces the total active power loss from 20.7138 kW to 10.7744 kW. This PV inclusion strategy also demonstrates a significant increase of 47.98% for the power loss reduction. The results also show that by adding more PV into the distribution network, the power loss reduction increases by 54.54% and 55.78% for two and three units of connected PV respectively.

The optimal PV location and sizing for the IEEE 33-bus network is shown in Table 3. A connection of one PV at Bus 6 with optimal sizing of 2572.5732 kW reduces the power loss from 203.0812 kW to 104.1595 kW. This proves that the network exhibits significant power loss reduction of 48.71%.

The results also show that by adding more PV into the system, the power loss reduction increases by 57.62% and 64.73% for two and three units of connected PV respectively.

To validate the reliability of the proposed optimal placement strategy for both IEEE 12 and 33-bus network, the voltage profiles with and without the presence of PV are plotted as in Figure 11 and Figure 12. The result shows that the installation of PV has significantly improved the voltage profiles for both IEEE 12 and 33-bus network, with respect to the increased number of the PV location.

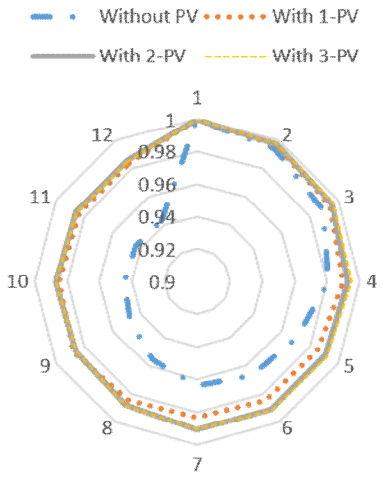


**Figure 11:** Voltage profile with and without PV for 12-bus network

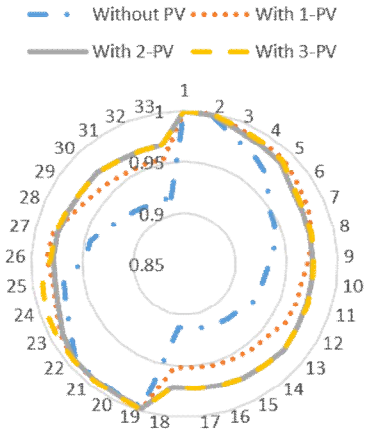


**Figure 12:** Voltage profile with and without PV for IEEE 33-bus network

For the IEEE 12-bus network with one PV location, the average voltage level is 0.98697 p.u. as compared to the average voltage level without PV which is 0.96346 p.u. As the number of PV was increased, the voltage level increased to 0.9900 p.u. and 0.9903 p.u. for two and three connected PV respectively. For the IEEE 33-bus network with one PV location, the average voltage level is 0.9484 p.u. as compared to the average voltage without PV which is 0.9484 p.u. The increased values of the average voltage level were recorded at 0.9804 p.u. and 0.9822 p.u. for two and three connected PV respectively. Hence, the overall results prove that the optimal PV location and sizing are important to enhance the system voltage profile.

## 4. CONCLUSION

This study presents Moth-Flame Optimization technique for optimal photovoltaic location and sizing in radial distribution network. The proposed method was tested on the IEEE 12 and 33-bus network. From the simulation results, it is proven that the optimized PV location and size in the distribution network could minimize the total active power loss and ensure the improvement of voltage profile to be within its acceptable range. It was found that the optimum PV location and sizing obtained using three different spiral techniques are comparable. However, the spiral techniques significantly affect the performance of the MFO algorithm in terms of consistency and convergence characteristics, where MFO-H demonstrates the best performance as compared to MFO-L and MFO-A.

## ACKNOWLEDGEMENT

The authors thank the Ministry of Education Malaysia (MOE) and the National University of Malaya (UKM) for supporting this work through FRGS research grant (FRGS/1/2018/TK04/UKM/02/12).

## REFERENCES

1. A. Colmenar-Santos, C. Reino-Rio, D. Borge-Diez, and E. Collado-Fernandez. **Distributed generation: A review of factors that can contribute most to achieve a scenario of DG units embedded in the new distribution networks,** *Renewable and Sustainable Energy Reviews*, Vol. 59, pp. 1130-1148, June 2016. https://doi.org/10.1016/j.rser.2016.01.023
2. G. V. K. Murthy, S. Sivanagaraju, S. Satyanarayana, and B. H. Rao. **Voltage stability analysis of radial distribution networks with distributed generation**, *International Journal on Electrical Engineering and Informatics*, Vol. 6, pp. 195-204, March 2014.
3. P. Paliwal, N. P. Patidar, and R. K. Nema. **Planning of grid integrated distributed generators: A review of technology, objectives and techniques,** *Renewable and Sustainable Energy Reviews*, Vol. 40, pp. 557-570, Dec. 2014.
4. P. S. Georgilakis, and N. D. Hatziargyriou. **Optimal distributed generation placement in power distribution networks: models, methods, and future research,** *IEEE Trans. on Power Systems*, Vol. 28, pp. 3420-3428, Jan. 2013. https://doi.org/10.1109/TPWRS.2012.2237043

5. K. Balamurugan, D. Srinivasan, abd T. Reindl. **Impact of distributed generation on power distribution systems**, *Energy Procedia*, Vol. 25, pp. 93-100, Sept. 2012.
6. P. Nijhawan, and A. S. Oberoi. **An innovative design of a solar-wind hybrid system,** *Int. Journal of Advanced Trends in Computer Science and Engineering*, Vol. 8, pp. 203-207, April 2019. https://doi.org/10.30534/ijatcse/2019/15822019
7. M. F. Akorede, H. Hizam, and E. Pouresmaeil. **Distributed energy resources and benefits to the environment**, *Renewable and sustainable energy reviews*, Vol. 14, pp. 724-734, Feb. 2010.
8. Z. A. Kamaruzzaman, A. Mohamed, and N. A. M. Kamari. **Effect of grid-Connected photovoltaic generator on dynamic voltage stability in power system,** *Jurnal Kejuruteraan*, Vol. 30, pp. 289-296, Oct. 2018.
9. M. A. Eltawil, and Z. Zhao. **Grid-connected photovoltaic power systems: Technical and potential problems - A review**, *Renewable and sustainable energy reviews*, Vol. 14, pp. 112-129, Jan. 2010.
10. R. Passey, T. Spooner, I. MacGill, M. Watt, and K. Syngellakis. **The potential impacts of grid-connected distributed generation and how to address them: A review of technical and non-technical factors**, *Energy Policy*, Vol. 39, pp. 6280-6290, Oct. 2011.
11. N. N. Mansor, S. A. Shaaya, I. Musirin, N. S Hannoon, Z. Mohamed, and M. K. M. Zamani. **Embedded flower pollination evolutionary programming based technique for voltage stability enhancement with distributed generation installation,** *Int. Journal of Advanced Trends in Computer Science and Engineering*, Vol. 8, pp. 387-393, Aug. 2019. https://doi.org/10.30534/ijatcse/2019/6881.32019
12. S. Angalaeswari, and K. Jamuna. **Optimal placement and sizing of real power supporting DG in radial distribution networks**, in *2015 IEEE Int. WIE Conference on Electrical and Computer Engineering (WIECON-ECE)*, Dhaka, 2015, pp. 342-345.
13. M. Abbagana, G. A. Bakare, and I. Mustapha. **Optimal placement and sizing of a distributed generator in a power distribution system using differential evolution**, in *Proc. 1st Int. Technology, Education and Environment Conf.*, Nigeria, 2011, pp. 536-549.
14. Z. Othman, S. I. Sulaiman, I. Musirin, A. M. Omar, and S. Shaari. **Optimal sizing stand alone photovoltaic system using evolutionary programming**, in *Proc. 9th Int. Conf. on Computer and Automation Engineering*, Sydney, 2017, pp. 302-306.
15. R. Orenge, M. Christopher Maina, and G. N. Nyakoe. **Optimal sizing and placement of solar photovoltaic based DGs in the IEEE 9 bus system using particle swarm optimization algorithm**, in *2018 IEEE PES/IAS Power Africa*, Cape Town, 2018, pp. 1-6.
16. A. Ymeri, and S. Mujovic. **Impact of photovoltaic systems placement, sizing on power quality in distribution network,** *Advances in Electrical and Computer Engineering*, Vol. 18, pp. 107-112, Nov. 2018. https://doi.org/10.4316/AECE.2018.04013
17. O. O. Oluwole. **Optimal allocation of distributed generation for power loss reduction and voltage profile improvement**, Ph.D dissertation, Univ. of Cape Town, South Africa, 2016.
18. M. Kefayat, A. L. Ara, and S. N. Niaki. **A hybrid of ant colony optimization and artificial bee colony algorithm for probabilistic optimal placement and sizing of distributed energy resources**, *Energy Conversion and Management*, Vol. 92, pp. 149-161, March 2015.
19. H. Doagou-Mojarrad, G. B. Gharehpetian, H. Rastegar, and J. Olamaei. **Optimal placement and sizing of DG (distributed generation) units in distribution networks by novel hybrid evolutionary algorithm**, *Energy*, Vol. 54, pp. 129-138, June 2013.
20. S. Mirjalili. **Moth-flame optimization algorithm: A novel nature-inspired heuristic paradigm,** *Knowledge-Based Systems*, Vol. 89, pp. 228-249, Nov. 2015.
21. M. Bahrami, O. Bozorg-Haddad, and X. Chu. **Moth-Flame Optimization (MFO) Algorithm**, in *Advanced Optimization by Nature-Inspired Algorithms*, Vol. 720, Singapore: Springer, 2018, pp. 131-141. https://doi.org/10.1007/978-981-10-5221-7_13
22. P. Singh, and S. Prakash. **Performance evaluation of moth-flame optimization algorithm considering different spiral paths for optical network unit placement in fiber-wireless access networks**, in *Int. Conf. on Information, Communication, Instrumentation and Control*, Indore, 2017, pp. 1-6.
23. G. M. Soliman, T. H. Abou-El-Enjen, E. Emary, and M. M. Khorshid. **A novel multi-objective moth-flame optimization algorithm for feature selection**, *Indian Journal of Science and Technology*, Vol. 11, pp. 1-13, Oct. 2018.
24. M. A Taher, S. Kamel, F. Jurado, and M. Ebeed. **An improved moth-flame optimization algorithm for solving optimal power flow problem**, *Int. Trans. on Electrical Energy Systems*, Vol. 29, pp. 1-28, March 2019. https://doi.org/10.1002/etep.2743
25. I. N. Trivedi, P. Jangir, S. A. Parmar, and N. Jangir. **Optimal power flow with voltage stability improvement and loss reduction in power system using Moth-Flame Optimizer**, *Neural Computing and Applications*, Vol. 30, pp. 1889-1904, Sept. 2018. https://doi.org/10.1007/s00521-016-2794-6